Parabolized Stability Equations analysis of nonlinear interactions with forced eigenmodes to control subsonic jet instabilities

Cite as: Phys. Fluids **27**, 084106 (2015); https://doi.org/10.1063/1.4928472
Submitted: 12 February 2015 • Accepted: 31 July 2015 • Published Online: 17 August 2015

Maxime Itasse, Jean-Philippe Brazier, Olivier Léon, et al.

PHYSICS OF FLUIDS **27**, 084106 (2015)

Parabolized Stability Equations analysis of nonlinear interactions with forced eigenmodes to control subsonic jet instabilities

Maxime Itasse,[a] Jean-Philippe Brazier,[b] Olivier Léon,[c] and Grégoire Casalis[d]
Onera - The French Aerospace Lab, F-31055 Toulouse, France

(Received 12 February 2015; accepted 31 July 2015; published online 17 August 2015)

Nonlinear evolution of disturbances in an axisymmetric, high subsonic, high Reynolds number hot jet with forced eigenmodes is studied using the Parabolized Stability Equations (PSE) approach to understand how modes interact with one another. Both frequency and azimuthal harmonic interactions are analyzed by setting up one or two modes at higher initial amplitudes and various phases. While single mode excitation leads to harmonic growth and jet noise amplification, controlling the evolution of a specific mode has been made possible by forcing two modes (m_1, n_1), (m_2, n_2), such that the difference in azimuth and in frequency matches the desired "target" mode $(m_1 - m_2, n_1 - n_2)$. A careful setup of the initial amplitudes and phases of the forced modes, defined as the "killer" modes, has allowed the minimizing of the initially dominant instability in the near pressure field, as well as its estimated radiated noise with a 15 dB loss. Although an increase of the overall sound pressure has been found in the range of azimuth and frequency analyzed, the present paper reveals the possibility to make the initially dominant instability ineffective acoustically using nonlinear interactions with forced eigenmodes. © *2015 AIP Publishing LLC.* [http://dx.doi.org/10.1063/1.4928472]

I. INTRODUCTION

If 30 yr of research and technological progress carried on engines have led to a jet noise decrease of more than 20 dB, the road to silence remains challenging for the aeronautical community. In Europe, the *Advisory Council for Aeronautics Research* (ACARE) has set an ambitious target to reduce the effective perceived noise by 50% from 2000 to 2020. To best meet those even more severe restrictions, the aerospace industry has performed some investigations in order to identify the noise sources leading to the intense acoustic radiation of the aircraft. Contrary to the interactions between the turbulence and the walls or the fan which are the dominant noise sources at landing, the high speed hot jet from the nozzle contributes for the largest part to the sound radiation during takeoff. A fine study of the underlying mechanisms is essential in the goal of developing sound-control strategies.

In this context, Lighthill[1] is considered as a pioneer of aeroacoustics. He was the first one who proposed an aerodynamically generated sound model by recasting the exact equations of fluid motion in the form of an inhomogeneous wave equation. Lighthill's eighth power law states that the acoustic power radiated by a jet is proportional to the eighth power of the jet speed and the square of its diameter. The law potential has been largely exploited by manufacturers with lower exit velocities and larger jet engines within the weight and size limits. New solutions have been sought and jet flow control has seemed promising over the past decades. Prediction of jet noise and

[a]Electronic mail: Maxime.Itasse@onera.fr
[b]Electronic mail: Jean-Philippe.Brazier@onera.fr
[c]Electronic mail: Olivier.Leon@onera.fr
[d]Electronic mail: Gregoire.Casalis@onera.fr

understanding of noise generation mechanisms have made significant progress but the exact role of turbulence is not yet completely understood.

In the late 1950s, where turbulence was considered purely chaotic, the experiment of Franklin and Foxwell[2] showed the existence of space-correlation in the random pressure field of a laminar jet, calling into question the non-deterministic behavior of the turbulence. Bradshaw *et al.*[3] confirmed these results for an initially laminar jet, highlighting large-scale coherent structures. In the case of turbulent mixing layers and jets, Mollo-Christensen *et al.*[4] and Crow and Champagne[5] also underlined the particular organization of the pressure disturbances in the form of spatially correlated wave-packets. Already, the possible significant role of these structures in bulk mixing and sound production was mentioned. Henceforth, the large-scale structures are recognized as a major component of the radiated far-field noise in the aft direction of high subsonic and supersonic jets.

By studying subsonic wave-packets, Crighton and Huerre[6] found that perturbation growth and decay generate supersonic components in the wavenumber spectra which radiate sound with superdirectivity in the aft of the jet. Recently, Cavalieri *et al.*[7] and Cavalieri and Agarwal[8] showed that temporal modulation and intermittency are also significant parameters in the generation of noise. On the whole, an increasing number of clues contributes to put emphasis on the role of large-scale structures in the radiated sound of jets. Excellent review papers are available in the scientific literature such as Tam[9] on jet noise research, Colonius and Lele[10] on computational aeroacoustics, and Jordan and Gervais[11] on experimental methods.

From an experimental point of view, as in the work of Suzuki and Colonius,[12] or through computational aeroacoustics, with Cavalieri *et al.*,[13] the study of these orderly structures may be carried out through different approaches. Despite significant progress on high-fidelity numerical simulations, Direct Numerical Simulation (DNS) and Large-Eddy Simulations (LESs) are still expensive. Stability theory offers a theoretical framework to study large-scale structures which have been identified as Kelvin-Helmholtz convective instabilities. A promising, but costly, method is the global stability analysis which provides access to the entire modes of a jet as realized by Nichols *et al.*[14] For accurately assessing the unstable modes describing the large-scale structures, more cost-effective methods are the local stability approaches.

The Parabolized Stability Equations (PSEs) are a generalization of the local Linear Stability Theory (LST). Originally conceived by Bertolotti and Herbert,[15] this method is able to capture non-parallel and nonlinear effects of slowly varying shear flows. First, Balakumar[16] and Yen and Messersmith[17] applied the linear PSE approach to cases of supersonic jets while high subsonic hot jets have been considered later by Bertolotti and Colonius.[18] If in supersonic case flow disturbances and the associated far-field acoustic radiation have been successfully captured, coupling with a propagation method is necessary in subsonic cases as highlighted by Piot *et al.*[19] Nonetheless, near-field comparisons with experiment are remarkable over a broad range of jet flows as in the works of Gudmundsson[20] and Gudmundsson and Colonius.[21] Recently, the linear PSE model has been applied to complex configurations. For example, Léon[22] and Léon and Brazier[23] have focused their work on dual-stream jets.

In order to control the jet noise, the main approach is to enhance the mixing mechanism. Chevrons, serrated or lobbed nozzles, continuous and pulsed micro-jets make it possible. It is now well established that high-amplitude impulsive or single-frequency excitation near the preferred mode of the jet can, to a certain extent, control the behavior of an axisymmetric shear layer and its radiated noise as in the experiments of Samimy *et al.*[24] and Kearney-Fischer *et al.*[25] But, because the instability wave can enhance mixing only if it continues to grow, the degree of jet spreading offered by single-frequency excitation remains limited. Indeed, beyond a "saturation" amplitude, further increases have no effect on the spreading as reported by Raman *et al.*[26]

In 1979, Ronneberger and Ackermann[27] underlined the arising of the difference-frequency mode $n_1 - n_2$ when forcing a fully turbulent jet simultaneously at two frequencies n_1, n_2. Then, interaction between the fundamental and subharmonic of the jet shear layer, referred as resonance or pairing, was largely investigated with simultaneous excitation of harmonically related acoustic tones. Arbey and Ffowcs Williams[28] exercised control on the process of harmonic generation by varying the phase between the two signals, sometimes virtually destroying the process. The effect of initial phase difference, Strouhal number pair, and amplitudes of the fundamental and subharmonics

tones was parametrically investigated by Raman and Rice.[29] Mankbadi[30] provided a theoretical analysis of the interaction between instability waves in a turbulent round jet while Suponitsky *et al.*[31] investigated linear and nonlinear mechanisms of sound generation in laminar subsonic jets by numerical resolution of the compressible Navier-Stokes equations. In particular, it was shown that low-frequency waves resulting from nonlinear interaction are more efficient in radiating sound when compared to linear instability waves radiating directly at the same frequencies. Experimentally, the possibility of controlling an artificially generated wave in the mixing layer of a jet has been investigated by Kopiev *et al.*,[32] where the theoretical conclusion that a time harmonic instability wave can be suppressed by an external acoustic wave with the properly chosen amplitude and phase has been verified. However, in the case of a natural turbulent jet, Rodriguez *et al.*[33] noticed that the richness of the modal spectrum reduced the efficiency of the difference-mode excitation.

As far as we know, jet noise reduction by mean of the control of naturally arising instability waves in a jet has never been demonstrated and learning how to properly force the jet in order to reduce, and not increase, the acoustic radiation is essential. Nonlinear PSE approach is perfectly suited to this issue because it allows to take into account modal resonances, in azimuth and in time. Malik and Chang[34] were the first to study helical-mode interaction, $m = \pm 1$, in a supersonic jet using nonlinear PSE. Disturbance saturation, spectrum filling, and large mean flow distortion downstream to the jet were the result of nonlinear interactions. The addition of an acoustic propagation model was undertaken by Cheung *et al.*[35] to investigate the influence of nonlinearity on the acoustic radiation of jets. Rolling-up vortices and coalescence were correctly reproduced in the near-field as well as the acoustic in the far-field.

Based on these works, the objective of the present paper is to rely on the proven ability of the hybrid PSE-acoustic propagation model to accurately capture the near and far-fields of jets to perform a parametric study for controlling the evolution of the dominating instability waves thereby influencing the radiated acoustic field. Although the intermittency of the wave-packets has a fundamental influence on sound emission, especially in a subsonic jet as mentioned by Cavalieri *et al.*,[7] the time-periodic forcing leads to phase-locked disturbances and thus the effect of jitter may not be a major issue here for the forced eigenmodes, following Cavalieri and Agarwal.[8] Despite this, nothing guarantees what the phase of the unforced modes will be. The extent of this analysis to natural broadband jets therefore suggests the need to control the initial phase of each mode altered by nonlinearity.

Such a study is carried out for two reasons. First, despite the fact that the large-scale structures are now recognized to play a significant role in the noise generation, the exact underlying mechanism is still not completely understood. Because the PSE approach allows to choose the retained azimuthal and frequency modes, as well as their relative initial amplitude and phase, isolating specific modes and evaluating their nonlinear contributions are made easier. With proper initial conditions, it is then possible to quantify how modes interact with one another. Second, with the recent development of active control techniques, such as plasma actuators, it is now possible to provide excitation signals at high amplitude and high frequency for flow control and noise reduction. However, an experimental parametric study over a broad range of forcing to reduce jet noise is time-consuming and costly. An efficient way to find relevant initial conditions is made possible through the use of nonlinear PSE. Indeed, as we know how nonlinear interactions occur, finding which modes to force at which amplitude and phase in order to minimize the near pressure field or the noise radiation is now feasible.

In the present paper, the nonlinear PSE approach is applied to a high subsonic hot jet with a Mach number $M_j = 0.7$ and a Reynolds number $Re_d = 4 \times 10^5$, corresponding to a previous LES computed by Huet.[36] For heated jets, as mentioned by Monkewitz and Sohn,[37] an absolute instability may be present. However, similarly to Gudmundsson,[20] due to the relatively low temperature ratio and the exhaust velocity, absolute instability is excluded in this work. Frequency and azimuthal modes interactions will be studied separately over a broad range of initial amplitudes and phases. The control of the dominant "target" mode will be made possible by increasing the amplitudes of "killer" modes. The optimization of the "killer" mode amplitudes and phases will lead to a decrease of the dominant unstable mode in the near-field as well as in the far-field.

The paper is organized as follows. Section II presents the nonlinear PSE and the Kirchhoff surface formulation. The mean flow, on which the PSE analysis will be conducted, is presented in Section III. Section IV explores first nonlinear interactions of axisymmetric modes at various frequencies while nonlinear contributions of azimuthal modes are analyzed and interpreted later.

II. INSTABILITY WAVE MODEL AND ACOUSTIC PROPAGATION

A. Parabolized stability equations

Nonlinear PSEs are used to evaluate the near-field flow disturbances generated by unstable waves in the jet shear layer. Literally, the vector of flow variables $\underline{q} = [u_x, u_r, u_\theta, \rho, p]^T$ is split into the sum of time-averaged $\overline{\underline{q}}$ and fluctuating $\underline{q}'$ components,

$$\underline{q}(x,r,\theta,t) = \overline{\underline{q}}(x,r) + \underline{q}'(x,r,\theta,t), \tag{1}$$

with x, r, θ the axial, radial, and azimuthal coordinates in the cylindrical reference frame and t the time variable. The usual perfect gas assumption is done so that the three velocity components, the density, and the pressure, as given in $\underline{q}$, are sufficient to characterize the flow. In the present paper, only round nozzles are considered, which makes possible the previous axisymmetric stationary form of the mean flow. A sum of Fourier modes is used to model the fluctuations, taking into account the symmetry in the azimuthal direction and assuming periodicity in time. If such an approach allows mode-to-mode interactions, a limitation to a finite number (m_{max}, n_{max}) of modes is necessary, which leads to series truncation,

$$\underline{q}'(x,r,\theta,t) = \sum_{n=-n_{max}}^{n_{max}} \sum_{m=-m_{max}}^{m_{max}} \underline{\tilde{q}}_{m,n}(x,r) \ \exp\ [i\,(m\theta - n\omega t)] + \underline{q}'', \tag{2}$$

with m the azimuthal wavenumber, ω the angular frequency, and n the harmonic frequency number. All the remaining unresolved modes are formally pulled together in $\underline{q}''$. It should be noted that even though negative frequencies ($n < 0$) are considered in Eq. (2), the disturbances are real-valued. Therefore, the computational effort can be reduced since only the modes with $n \geq 0$ need to be solved by imposing the following condition:

$$\underline{\tilde{q}}_{-m,-n} = \underline{\tilde{q}}^{\dagger}_{m,n}, \tag{3}$$

where † refers to the complex conjugate.

Assuming the mean flow $\overline{\underline{q}}$ to be weakly non-parallel in the streamwise direction x, the modal function $\underline{\tilde{q}}_{m,n}$ is decomposed into a slowly varying shape function in the axial x-direction $\underline{\hat{q}}_{m,n}$ and a rapidly varying wave-like part $\mathcal{A}_{m,n}$ as developed by Bertolotti and Herbert,[15]

$$\underline{\tilde{q}}_{m,n}(x,r) = \underline{\hat{q}}_{m,n}(x,r)\,\mathcal{A}_{m,n}(x) = \underline{\hat{q}}_{m,n}\gamma_{m,n} \ \exp\ \left(i \int_{x_0}^{x} \alpha_{m,n}(\xi)\,d\xi\right), \tag{4}$$

$$\text{with } \gamma_{m,n} = \varepsilon_{m,n} \ \exp\ (i\,\phi_{m,n}), \tag{5}$$

where $\alpha_{m,n}$ is the complex axial wavenumber and x_0 the initial axial location. $\varepsilon_{m,n}$ is the maximum amplitude of the streamwise disturbance velocity $\hat{u}_{x_{m,n}}$ occurring at a radius where $\phi_{m,n}$ is defined as the phase, both imposed at x_0.

Because the instability waves studied result from the inflectional mean profile of the jet shear layer, the viscous dissipation is assumed to have minor effects on their evolution for such flows at high Reynolds numbers and is neglected. Thus, the normal modes Eqs. (2) and (4) are introduced into the compressible inviscid continuity, momentum, and energy equations of a perturbed flow. Subtracting the terms corresponding to the mean flow yields the governing equations,

$$\mathcal{L}_{m,n}\{\underline{\hat{q}}_{m,n}\} = A_{m,n}\underline{\hat{q}}_{m,n} + B\frac{\partial \underline{\hat{q}}_{m,n}}{\partial x} + C\frac{\partial \underline{\hat{q}}_{m,n}}{\partial r} = -\frac{\mathcal{F}_{m,n}}{\mathcal{A}_{m,n}} - \frac{\mathcal{F}''_{m,n}}{\mathcal{A}_{m,n}}. \tag{6}$$

For the sake of clarity, the present system of equations is called the PSE, even though, unlike the original PSE, they are derived from the Euler equations, instead of the Navier-Stokes equations.

The operator $\mathcal{L}_{m,n}$ is linear and depends only on the mean flow variables $\overline{q}$, the axial wavenumber $\alpha_{m,n}$, the angular frequency ω, and the first-order derivatives. On the right-hand side, the nonlinear term $\mathcal{F}_{m,n}$ involves products of the resolved azimuthal and frequency modes. They are evaluated in the time domain and transformed back into the frequency domain by means of FFT. The function $\mathcal{F}''_{m,n}$ gathers the contributions resulting from nonlinear interactions involving unresolved modes. It will be neglected here, but it should be pointed out that due to the series truncation uncertainty, $\mathcal{F}''_{m,n}$ is not necessarily negligible. Further insight on that issue can be found in Rodriguez *et al.*[33]

Similarly to the Parabolized Navier-Stokes (PNSs) equations, the system exhibits ellipticity due to $\partial\hat{p}/\partial x$, as mentioned by Haj-Hariri.[38] Following the approach developed by Vigneron *et al.*,[39] sufficient conditions to make the system parabolic were sought by splitting $\partial\hat{p}/\partial x$ in two terms in the x-momentum equation,

$$\frac{\partial \hat{p}}{\partial x} = w\frac{\partial \hat{p}}{\partial x} + (1-w)\frac{\partial \hat{p}}{\partial x}. \tag{7}$$

If the first right-hand side term of Eq. (7) is kept while the second one is considered as a source term, the parabolicity condition provides a set of equations,

$$\begin{cases} \overline{\rho}\, M^2\, \overline{u}_r^2 < 1 \\ w \leq \dfrac{\overline{\rho}\, M^2\, \overline{u}_x^2}{1-\overline{\rho}\, M^2\, \overline{u}_r^2} \end{cases}. \tag{8}$$

with M the reference Mach number at the jet exit. The first condition requires the PSE approximation to be used only with slowly diverging jet, since $\overline{u}_r$ needs to be small enough. The second one indicates the maximum fraction of $\partial\hat{p}/\partial x$ that can be retained in the equations while maintaining them parabolic in the streamwise direction. One can notice that the effect of $\partial\hat{p}/\partial x$ is completely neglected for incompressible jets, where $w(M=0)=0$, and is progressively included as the compressibility effects increase. Practically, w is evaluated as

$$w = \min\left[1, \frac{\rho M^2 \overline{u}_x^2}{1-\rho M^2 \overline{u}_r^2}\right]. \tag{9}$$

The PSEs so obtained are now parabolic and can be solved by a computationally efficient streamwise marching technique. However, this parabolicity can be questioned for the normalization condition which is introduced in the following.

In Eq. (4), streamwise variations can be either absorbed in the axial wavenumber $\alpha_{m,n}$ or in the eigenfunction $\underline{\hat{q}}_{m,n}$ component. A closure relationship on the kinetic energy is then employed individually for each mode to remove this ambiguity, as proposed by Bertolotti and Herbert,[15]

$$N_{m,n} = \int_0^\infty \underline{\hat{q}}^\dagger_{m,n} \frac{\partial \underline{\hat{q}}_{m,n}}{\partial x}\, dr = \int_0^\infty \left(\hat{u}_x^\dagger \frac{\partial \hat{u}_x}{\partial x} + \hat{u}_r^\dagger \frac{\partial \hat{u}_r}{\partial x} + \hat{u}_\theta^\dagger \frac{\partial \hat{u}_\theta}{\partial x}\right) dr = 0. \tag{10}$$

At $r=0$, many terms in the PSE are singular, especially in $\mathcal{F}_{m,n}$. Relying on the symmetry about the x-axis, the following boundary conditions are applied,

$$\begin{cases} \dfrac{\partial \hat{u}_x}{\partial r} = \hat{u}_r = \hat{u}_\theta = \dfrac{\partial \hat{\rho}}{\partial r} = \dfrac{\partial \hat{p}}{\partial r} = 0 & : \quad \text{for } m = 0, \\ \hat{u}_x = \dfrac{\partial \hat{u}_r}{\partial r} = \dfrac{\partial \hat{u}_\theta}{\partial r} = \hat{\rho} = \hat{p} = 0 & : \quad \text{for } |m| = 1, \\ \hat{u}_x = \hat{u}_r = \hat{u}_\theta = \hat{\rho} = \hat{p} = 0 & : \quad \text{for } |m| \geq 2. \end{cases} \tag{11}$$

In the far-field $r \to +\infty$, considering a medium at rest and neglecting the streamwise derivatives $\partial\hat{u}_x/\partial x$ and $\partial\hat{p}/\partial x$, the PSE simplify to a second order homogeneous differential Bessel

equation for the pressure,

$$\frac{\partial^2 \hat{p}}{\partial r^2} + \frac{1}{r}\frac{\partial \hat{p}}{\partial r} + \left(\overline{\rho} n^2 \omega^2 M^2 - \frac{m^2}{r^2} - \alpha^2\right)\hat{p} = 0. \tag{12}$$

The pressure shape function takes far away from the jet the form of a Hankel function of the first kind and order m,

$$\hat{p}(x,r) = H_m^{(1)}(ir\lambda(x)), \tag{13}$$

with $\lambda^2 = \alpha^2 - \overline{\rho} n^2 \omega^2 M^2$ such that $Re(\lambda) > 0$. Hankel-based boundary conditions are then applied at $r = 15d$, where d is the diameter of the nozzle, similarly to Piot *et al.*[19]

The discrete system of Eq. (6) is obtained by combining a fourth-order central compact finite difference scheme proposed by Gamet *et al.*[40] in the radial direction and an implicit first-order backward Euler scheme with a step size $\Delta x = x_i - x_{i-1}$ in the streamwise direction,

$$\left(A^i_{m,n} + \frac{B^i}{\Delta x} + C^i \cdot D^i\right)\underline{\hat{q}}^i_{m,n} = \frac{B^{i-1}}{\Delta x}\underline{\hat{q}}^{i-1}_{m,n} - \frac{\mathcal{F}^i_{m,n}}{\mathcal{A}^i_{m,n}}, \tag{14}$$

with D^i the radial differentiation matrix such that $\partial \underline{\hat{q}}^i_{m,n}/\partial r = D^i \cdot \underline{\hat{q}}^i_{m,n}$.

Initial conditions for the PSE marching procedure are obtained through the local linear parallel stability theory. However, contrary to linear PSE, the initial amplitudes and phases of the modes, defined in Eq. (5), are key parameters here as discussed later on. The shape functions of all the $\underline{\hat{q}}_{m,n}$ modes are computed solving iteratively discrete system Eq. (14). The axial wavenumbers $\alpha_{m,n}$ are updated at each iteration using a Newton-Raphson method based on the normalization condition Eq. (10) as in Léon and Brazier.[41]

B. Cylindrical Kirchhoff surface formulation

As observed by Cheung *et al.*,[35] even though the PSE approach is able to accurately capture the perturbations inside the jet, it will fail in the appraisal of the acoustic radiation. However, as mentioned by Suzuki and Colonius,[12] the hydrodynamic PSE modes remain valid and dominant outside of the mixing layer on a limited radius range called the hydrodynamic area, where the mean flow is nearly irrotational and at rest. A cylindrical Kirchhoff surface positioned in that area will allow to reconstruct the far-field acoustic radiation associated with hydrodynamic fluctuations, similarly to Balakumar[16] and Gudmundsson and Colonius.[42]

Assuming a medium at rest outside of the jet, the pressure fluctuations satisfy the wave equation,

$$\frac{\partial^2 \tilde{p}_{m,n}}{\partial r^2} + \frac{\partial^2 \tilde{p}_{m,n}}{\partial x^2} + \frac{1}{r}\frac{\partial \tilde{p}_{m,n}}{\partial r} + \left(\overline{\rho} M^2 n^2 \omega^2 - \frac{m^2}{r^2}\right)\tilde{p}_{m,n} = 0, \tag{15}$$

where the pressure disturbances calculated by the PSE are used as boundary conditions at the radial location r_K of the Kirchhoff surface. A Fourier transform in the axial direction leads to a Bessel differential equation whose solution can be expressed by means of first-kind Hankel functions,

$$\tilde{p}_{m,n}(x,r) = \int_{-\infty}^{\infty} \tilde{p}^{(0)}_{m,n}(\eta)\frac{H_m^{(1)}(ir\lambda_K)}{H_m^{(1)}(ir_K\lambda_K)} e^{i\eta x} d\eta, \tag{16}$$

$$\text{where } \lambda_K^2 = \rho_\infty M^2 n^2 \omega^2 - \eta^2 \text{ with } \mathrm{Re}(\lambda_K) > 0 \tag{17}$$

and with $\tilde{p}^{(0)}_{m,n}$ the axial Fourier transform of the pressure fluctuation on the Kirchhoff surface. The total pressure fluctuation in the far-field is then rebuilt based on the previous modal decomposition,

$$p'(x,r,\theta,t) = \sum_{n=-n_{max}}^{n_{max}} \sum_{m=-m_{max}}^{m_{max}} \tilde{p}_{m,n}(x,r)\ \exp\ i\,(m\theta - n\omega t). \tag{18}$$

C. Validation

A validation of the linear PSE code and of the Kirchhoff surface strategy has been previously realized by Léon[23,41] and Brazier *et al.*,[43] for various jet configurations ranging from the incompressible jet of Yen and Messersmith[17] to the supersonic jet experimentally studied by Troutt and McLaughlin.[44] Both near-field and far-field pressure distributions were correctly predicted for various frequencies and azimuthal wavenumbers. The results supported the validity of the linear PSE code and of the Kirchhoff surface formulation.

Since numerical simulations of turbulent jets with forced eigenmodes are uncommon, in order to validate the computation of the right-hand side term $\mathcal{F}_{m,n}$ of Eq. (6), which contains the nonlinearities, two approaches have been used and compared.

The first previously mentioned approach consists in computing the nonlinear forcing terms in the time domain and transforming them back to the frequency domain by a Fourier transform. A second method allows to find an analytical solution of $\mathcal{F}_{m,n}$ by identifying the product of series as a Cauchy product. The contributions of the second-order nonlinear terms on each mode are calculated analytically. The third-order nonlinear terms are not taken into account in this computation. For the optimized case mentioned later in Sec. IV E, a comparison of $\mathcal{F}_{0,2}^{(i)}$ real and imaginary parts computed by Fourier transform (∘) and analytically (–) at $x/d = 3.0$ is reported in Fig. 1. The exponent (i) refers, respectively, to continuity, x-momentum, r-momentum, θ-momentum, and energy equations. Because only axisymmetric modes are considered in that specific example, $\mathcal{F}_{0,2}^{(4)}$ equals zero. All results match perfectly for any x/d, then it is assumed that nonlinear terms are correctly estimated.

III. MEAN FLOW COMPUTATION

Thereafter, a round nozzle with an exhaust diameter d of 80 mm previously studied by Muller *et al.*[45] and Huet[36] is considered. The jet characteristics are the Mach number $M = U_j/c_j = 0.7$, where c_j stands for the sound speed and $U_j = 404$ m s^{-1} is the jet velocity, both at the centerline of the nozzle exit section. The temperature in the core region is $T_j = 830$ K and the Reynolds number based on the exit conditions is $Re_d = 4 \times 10^5$. The ambient pressure and temperature are $p_0 = 101\,325$ Pa and $T_0 = 280$ K, respectively.

Unsteady flow field computation was performed by Huet[36] using LES with a Smagorinsky subgrid-scale model. An O-shaped conformal structured grid of 30×10^6 cells has been used to model the nozzle and the jet. To provide accuracy close to the walls, the grid is densified near the walls to resolve thickened boundary layers. Of particular interest was the influence of boundary layer resolution to numerically reproduce initially turbulent jets. It was found necessary to seed turbulence inside the nozzle. Thus, uniform stagnation pressure and temperature values were

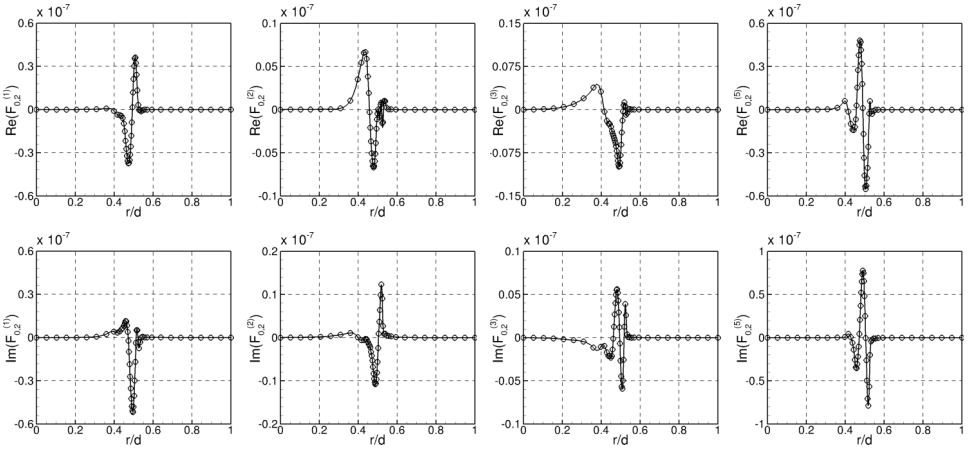

FIG. 1. Real and imaginary part of $\mathcal{F}_{0,2}^{(i)}$ computed by Fourier transform (∘) and analytically (–) at $x/d = 3.0$.

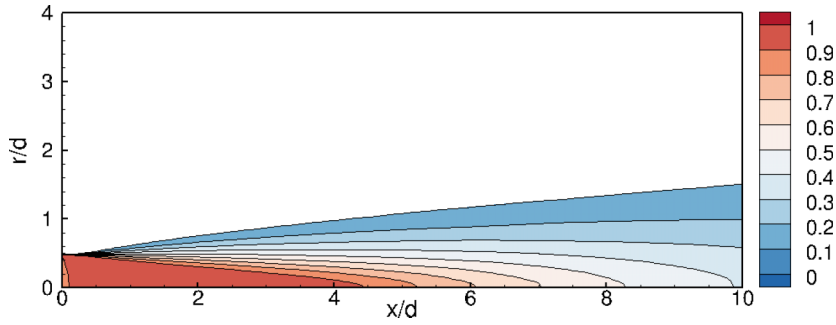

FIG. 2. Mean axial velocity contour from the LES.

exclusively imposed at the inlet and the boundary layers were let run their course. Time integration was made with a first-order implicit time scheme concurrently with a second-order upwind space discretization scheme to solve the Navier-Stokes equations. To perform mean flow averaging, the simulation was run with a time step of $\Delta t = 2 \times 10^{-7}$ s up to a physical time of 60 ms or to a dimensionless time of 300 convective time units d/U_j, which was thought to be long enough to ensure a sufficient statistical convergence of the flow field.

In the case of turbulent flows, taking the mean flow as the base flow in stability analysis may be unsuitable, as mentioned by Bagheri *et al.*[46] However, as shown by Piot *et al.*,[19] Brazier *et al.*[43] and Gudmundsson and Colonius[21] with linear PSE and by Rodriguez *et al.*[33] with nonlinear PSE, applying stability theory on that "base flow" leads to good results in comparison with experiments, at least up to the end of the core region. In the present paper, failing any other alternative, the mean flow computed by the LES will also be used as a base flow. The mean axial velocity contour from the LES is presented in Fig. 2.

It is also worth emphasizing that nonlinear interactions of the instability waves may produce zero-frequency modes ($n = 0$), representing a distortion of the mean flow. For laminar weakly forced jets, Salgado *et al.*[47] noted that mean flow correction did not induce much change in the behaviour of the modes, while it became a more important factor when a larger number of modes are affected by nonlinearity. Malik and Chang[34] also pointed out that this effect was mostly located downstream the potential core. In the case of a natural turbulent jet, the mean flow computed by the LES already includes the zero-frequency modes and computing them again with PSE would therefore be redundant, as mentioned in Rodriguez *et al.*[33] In the present analysis, where a specific forcing of modes is investigated, consideration of the mean flow distortion would perhaps be necessary but that would require to extract the base flow directly from the LES computation, which was not done here. However, this choice could be reconsidered in future work.

According to the above-mentioned remarks, we think that our results are valid before the end of the core region, but remain more questionable downstream.

IV. NONLINEAR INTERACTIONS ANALYSIS

The PSE model, presented in Sec. II A, is used here to understand how modes interact with one another on a realistic jet configuration. In order to clarify the following analysis, the main steps of the process are synthesized here.

For the natural unforced jet, the most amplified instabilities are axisymmetric ($m = 0$) in a frequency band around $St = 0.40$. As well, the radiated sound is broadband and predominates mainly downstream of the jet over the same frequency range. The purpose of this study is to alter the behavior of a specific mode. Therefore, the mode on which control is needed, designated as the "target" mode, will be the axisymmetric mode ($m = 0$) at $St = 0.40$.

As a first step, the analysis will be limited to frequency harmonic interactions. Identical initial amplitudes and phases will be set to all modes except one or two, the "killer" modes. Pure tone excitation will induce harmonic growth and jet noise amplification, which is not in agreement with

the current purpose. However, forcing two modes at higher initial amplitudes will only influence the difference-frequency mode. Alteration of the dominant mode development is then made possible. Near pressure field of the "target" mode will be minimized through a careful scan of initial amplitudes and phases of the "killer" modes. Far-field noise of the initially dominant mode will be reduced drastically whereas the high frequencies will be increased. Shifting "killer" modes to even higher frequencies will conclude the analysis of frequency nonlinear interactions.

Finally, the overall same process will be applied to azimuthal modes interactions at various frequencies, exciting two specific "killer" modes. As previously, bimodal excitation will be found relevant to alter "target" mode development, revealing at the same time not only the difference-frequency but also the difference-azimuth phenomenon.

A. Effect of the initial modes amplitudes

Six axisymmetric modes are considered with frequencies ranging from $St = 0.20$ to 1.20 by step of 0.20 ($n_{max} = 6$). Even though accurate measurements at the nozzle were not performed on that configuration, relevant initial amplitudes are needed. As mentioned by Rodriguez *et al.*,[33] in the case of a turbulent jet where a broad spectrum of fluctuations exists, the order of magnitude of initial amplitudes must be the same for a large number of modes. Taking as a reference their measurements on a cold subsonic jet at $M = 0.9$, initial pressure amplitudes were found to be between 0.01 and 0.1 Pa corresponding to a dimensionless initial amplitude factor $\varepsilon_{m,n} = 10^{-5}$ following Eq. (5).

Three different cases are considered next, looking at the effect of the initial modes amplitudes. The same initial amplitudes and phases are assigned to all the modes for various initial conditions ranging from 1×10^{-5} to 1×10^{-3} as summarized in Table I. The results are presented in Fig. 3 where the N factor is used to compare the axial evolution of the modes,

$$\mathrm{N} = \ln\left(\frac{A(x)}{A(x_0)}\right), \tag{19}$$

with $A(x) = \left[\int_0^\infty \left(|\hat{u}_x|^2 + |\hat{u}_r|^2 + |\hat{u}_\phi|^2\right) dr\right]^{1/2}$ the root mean square velocity fluctuation. Nonlinear effects will be highlighted by the disparity between linear and nonlinear curves.

One can observe that for low initial amplitudes, the linear and nonlinear computations match perfectly. The nonlinear interactions have no effect on the modes evolution. On the other hand, discrepancies appear at higher amplitudes. Thus, for $\varepsilon_{m,n} = 10^{-3}$, slight modifications in the evolution of the modes $n = 2,4,5$, and 6 are noticeable while the mode $n = 1$ is significantly changed. The mode $n = 3$ seems to be unaltered under that specific initial conditions. Weak nonlinear effects are also mentioned by Salgado *et al.*[47] at similar initial amplitudes.

The main difficulty is to understand why one mode is changed by nonlinearity and another one is not. In the following discussion, a step-by-step analysis is proposed to clarify the underlying mechanism of frequency harmonic interactions with the aim to control the dominant mode (0,2) corresponding to $St = 0.4$.

B. Single frequency excitation

In this section, single frequency excitation effect is analyzed. The present purpose is not to provide an exact representation of the jet but rather to investigate nonlinear interaction of subsonic jet instabilities with forced eigenmodes. In order to isolate phenomena, all the modes are then

TABLE I. Initial amplitudes of modes referring to Fig. 3.

Case	$\varepsilon_{0,1}$ ($St = 0.2$)	$\varepsilon_{0,2}$ ($St = 0.4$)	$\varepsilon_{0,3}$ ($St = 0.6$)	$\varepsilon_{0,4}$ ($St = 0.8$)	$\varepsilon_{0,5}$ ($St = 1.0$)	$\varepsilon_{0,6}$ ($St = 1.2$)
A1 (○)	1×10^{-5}	1×10^{-5}	1×10^{-5}	1×10^{-5}	1×10^{-5}	1×10^{-5}
A2 (●)	1×10^{-4}	1×10^{-4}	1×10^{-4}	1×10^{-4}	1×10^{-4}	1×10^{-4}
A3 (△)	1×10^{-3}	1×10^{-3}	1×10^{-3}	1×10^{-3}	1×10^{-3}	1×10^{-3}

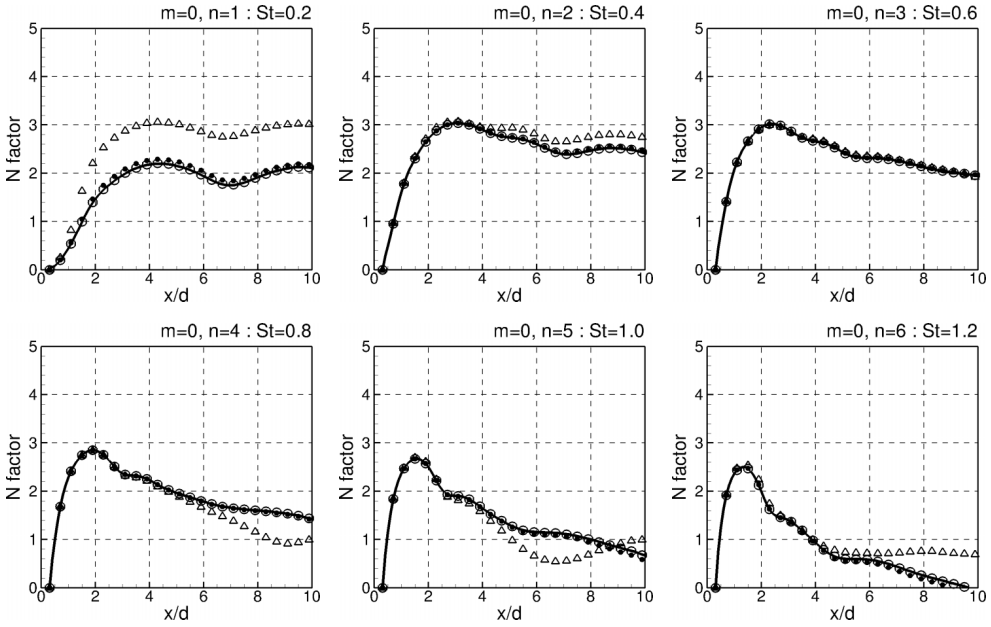

FIG. 3. N factor comparison for all modes between nonlinear computations at various initial amplitudes $\varepsilon_{m,n} = 10^{-5}$ (○); 10^{-4} (●); 10^{-3} (△); and linear PSE (–).

initialized at the same deliberately low initial amplitude of $\varepsilon_{m,n} = 1 \times 10^{-7}$, similarly to Salgado *et al.*[47] The $St = 0.4$ is an exception with an initial amplitude increased to $\varepsilon_{0,2} = 1 \times 10^{-5}$ and $\varepsilon_{0,2} = 1 \times 10^{-4}$ to simulate the effect of forcing the dominant mode, as mentioned in Table II. Results are reported in Fig. 4 where the N factor is used to illustrate the nonlinear effects.

On the one hand, with $\varepsilon_{0,2} = 1 \times 10^{-5}$, only slight changes appear on the $St = 0.8$ mode, which corresponds to the first harmonic of the forced mode. All the remaining modes are kept unaltered by the nonlinear interactions. On the other hand, as the initial amplitude of the forced mode is increased, the discrepancies previously revealed on the $St = 0.8$ become clearly significant with a sharp increase of the N factor. As the first harmonic becomes large enough, the second one $St = 1.2$ starts to be also affected. The leftover modes are still insensitive to the forced mode.

As reported by Bechert and Pfizenmaier,[48] above a certain excitation level, due to harmonics growth, the broadband jet noise can then be amplified considerably by a pure tone excitation. However, with a view to controlling dominant mode, forcing low frequency modes at high amplitudes is not conceivable. A more efficient mechanism is needed.

C. Difference-frequency mode

In 1979, Ronneberger and Ackermann[27] ran experiments on a turbulent jet to quantify the effect of nonlinear interactions of instability waves on the radiated sound. By exciting a jet at two frequencies n_1, n_2, they found that the combination frequencies $n_1 - n_2$, $n_1 + n_2$, $2n_1 - n_2$, and $2n_2 - n_1$ exhibit wave-like character in the near-field. In addition, the difference-frequency $n_1 - n_2$ predominates over other combination frequencies in the far-field, with a distinct directivity.

TABLE II. Initial amplitudes of modes referring to Fig. 4. Boldface values refer to the forced mode initial conditions.

Case	$\varepsilon_{0,1}$ ($St = 0.2$)	$\varepsilon_{0,2}$ ($St = 0.4$)	$\varepsilon_{0,3}$ ($St = 0.6$)	$\varepsilon_{0,4}$ ($St = 0.8$)	$\varepsilon_{0,5}$ ($St = 1.0$)	$\varepsilon_{0,6}$ ($St = 1.2$)
B1 (○)	1×10^{-7}	$\mathbf{1 \times 10^{-5}}$	1×10^{-7}	1×10^{-7}	1×10^{-7}	1×10^{-7}
B2 (●)	1×10^{-7}	$\mathbf{1 \times 10^{-4}}$	1×10^{-7}	1×10^{-7}	1×10^{-7}	1×10^{-7}

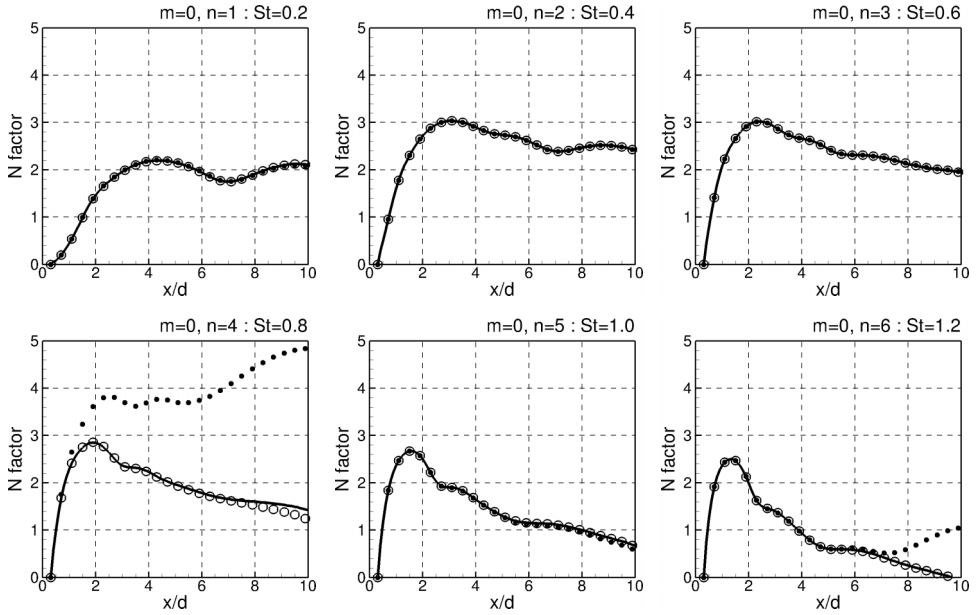

FIG. 4. Effect of forcing one frequency, mode (0,2), at a higher amplitude; $\varepsilon_{0,2} = 10^{-5}$ (○); 10^{-4} (•); linear PSE (–).

This process is here investigated numerically. The initial amplitude of $\varepsilon_{m,n} = 1 \times 10^{-7}$ remains assigned to all modes while the two frequencies $St = 0.8$ and $St = 1.2$ are forced at higher initial amplitudes. Three different initial amplitudes are analyzed $\varepsilon_{0,4} = \varepsilon_{0,6} = 1 \times 10^{-5}$ (○), 2×10^{-5} (•), and 4×10^{-5} (△) as referred in Table III. The N factor of all the modes under these configurations is reported in Fig. 5.

As expected, by forcing two specific frequencies, only the difference-frequency mode $St = 0.4$ is affected. If the maximum of the amplification factor is increased by 30%, its location, around $x/d = 3.0$, is not altered.

The use of difference-mode interaction may then be promising in order to control jet instabilities and possibly reduce noise radiation if the pressure field is altered favorably. The two forced frequencies, where energy is injected in to alter the behavior of a specific "target" mode, are qualified as "killer" modes. However, as shown above, the N factor of the difference-frequency mode is very sensitive to the initial amplitudes of the forced modes.

In the next paragraph, attention will be paid to the effect of the initial amplitudes and phases of the "killer" modes on the near pressure field.

D. Initial phase effects in the near-field

If the N factor is an effective parameter to quantify the influence of nonlinear interactions on modes, the pressure field remains the starting point of any acoustic analysis. As an extension of the previous case C2 (○), the pressure amplitude $|p'_{0,2}|$ of the mode (0,2) along the line $r/d = 0.5$ is reported on the top left side of Fig. 6. It should be noted that the two "killer" frequencies $St = 0.8$ and

TABLE III. Initial amplitudes of modes referring to Fig. 5. Boldface values refer to the forced modes initial conditions.

Case	$\varepsilon_{0,1}$ ($St = 0.2$)	$\varepsilon_{0,2}$ ($St = 0.4$)	$\varepsilon_{0,3}$ ($St = 0.6$)	$\varepsilon_{0,4}$ ($St = 0.8$)	$\varepsilon_{0,5}$ ($St = 1.0$)	$\varepsilon_{0,6}$ ($St = 1.2$)
C1 (○)	1×10^{-7}	1×10^{-7}	1×10^{-7}	$\mathbf{1 \times 10^{-5}}$	1×10^{-7}	$\mathbf{1 \times 10^{-5}}$
C2 (•)	1×10^{-7}	1×10^{-7}	1×10^{-7}	$\mathbf{2 \times 10^{-5}}$	1×10^{-7}	$\mathbf{2 \times 10^{-5}}$
C3 (△)	1×10^{-7}	1×10^{-7}	1×10^{-7}	$\mathbf{4 \times 10^{-5}}$	1×10^{-7}	$\mathbf{4 \times 10^{-5}}$

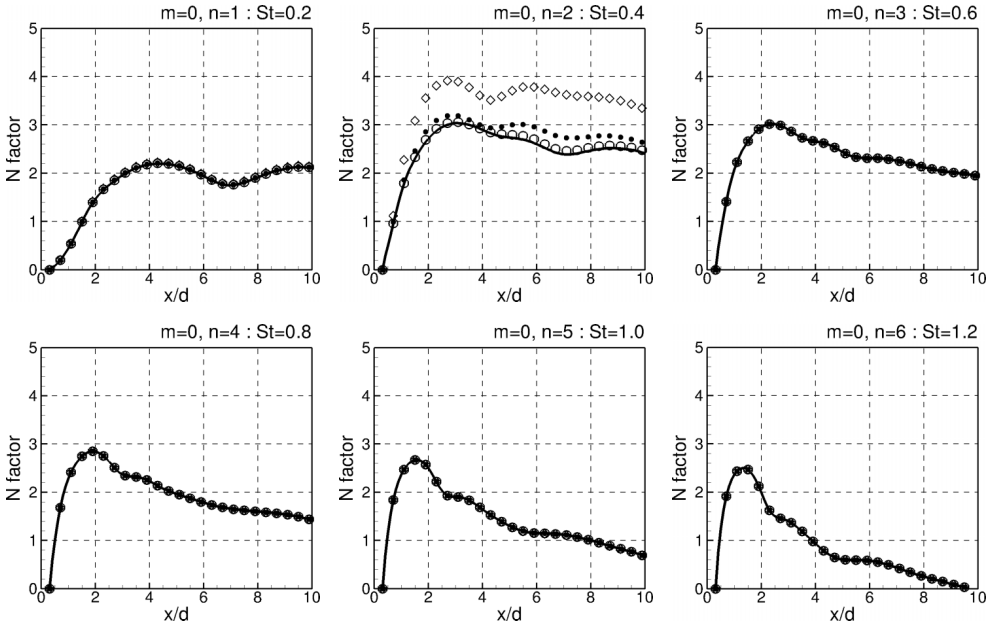

FIG. 5. Effect of forcing two high frequencies, modes (0,4) and (0,6), at higher initial amplitudes; $\varepsilon_{0,4} = \varepsilon_{0,6} = 1\times10^{-5}$ (∘); 2×10^{-5} (•); 4×10^{-5}(△); linear PSE (–).

$St = 1.2$ influence exclusively the "target" mode $St = 0.4$; consequently, only the pressure amplitude of the latter will be represented in the following figures. With $\varepsilon_{0,4} = \varepsilon_{0,6} = 2\times10^{-5}$ (∘), even though the peak location remains the same, its value is increased by more than 20%. The acoustic radiation generated by the mode $St = 0.4$ may intensify as well which would defeat the purpose.

Until now, a missing parameter was the initial phase of the modes which has been found relevant in the process of resonance or pairing by Arbey and Ffowcs Williams.[28] By varying the phase between two signals at harmonically related frequencies, control was exercised on both harmonic

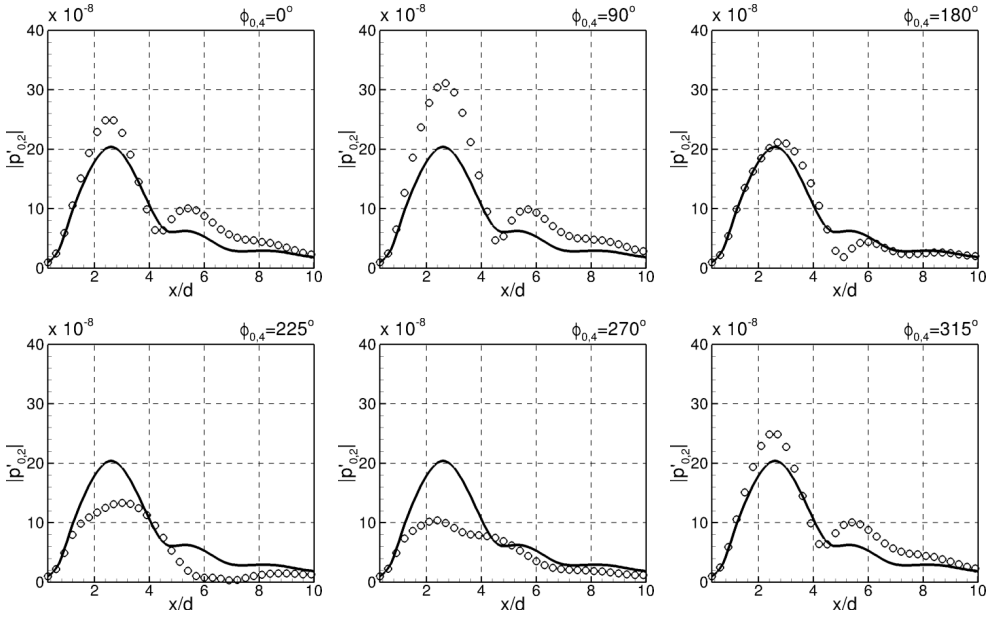

FIG. 6. Pressure amplitude of the "target" mode (0,2) along the line $r/d = 0.5$ when forcing the modes (0,4) and (0,6) at $\varepsilon_{0,4} = \varepsilon_{0,6} = 2\times10^{-5}$ (∘) for various initial phases of the mode (0,4); (–) linear PSE.

TABLE IV. Various initial amplitudes of modes leading to the same results in the near-field. Boldface values refer to the forced modes initial conditions.

Case	$\varepsilon_{0,1}$ ($St = 0.2$)	$\varepsilon_{0,2}$ ($St = 0.4$)	$\varepsilon_{0,3}$ ($St = 0.6$)	$\varepsilon_{0,4}$ ($St = 0.8$)	$\varepsilon_{0,5}$ ($St = 1.0$)	$\varepsilon_{0,6}$ ($St = 1.2$)
E1	1×10^{-7}	1×10^{-7}	1×10^{-7}	$\mathbf{2 \times 10^{-5}}$	1×10^{-7}	$\mathbf{4 \times 10^{-5}}$
E2	1×10^{-7}	1×10^{-7}	1×10^{-7}	$\mathbf{4 \times 10^{-5}}$	1×10^{-7}	$\mathbf{2 \times 10^{-5}}$
E3	1×10^{-7}	1×10^{-7}	1×10^{-7}	$\mathbf{1 \times 10^{-5}}$	1×10^{-7}	$\mathbf{8 \times 10^{-5}}$

and subharmonic generation. Despite the fact that enhancing jet mixing by high-amplitude excitation has been well documented, the significance of the phase difference in the control of naturally arising instability waves in a jet and its part in the far-field noise is not known. It is therefore legitimate to ask whether any phase difference between the "killer" modes will change the pressure distribution of the "target" mode.

The phase influence of the forced mode (0,4) on the pressure amplitude of the target mode (0,2) is represented in Fig. 6. All the remaining modes are left with their previous initial conditions, such as the initial phase of the mode (0,6) which remains at zero. The phase impact on the pressure amplitude peak is obvious and promising. Indeed, if the peak value can be increased by 50% when forcing the initial phase of the mode (0,4) at $\phi_{0,4} = 90°$, most importantly it can be reduced by 50% when $\phi_{0,4} = 270°$. It also highlights the great significance of the relative initial phase of the modes when nonlinear interactions occur.

A way to reduce the efficiency of a dominant mode in the near-field should be to amplify two higher frequencies so that the difference-frequency mode corresponds to the "target" mode and sets their initial phases in order to reduce its pressure peak value.

E. "Target" mode pressure peak minimization

An optimum in terms of initial amplitudes and phases of the "killer" modes is sought with the aim of reducing as much as possible the pressure peak value of the "target" frequency. After running multiple cases, it is not the initial amplitude of each mode set apart which was found relevant, but their product. As an example, Table IV summarizes three different cases where the initial amplitude product remains constant. The results, not presented here, superimposed perfectly between themselves in the near-field and thus, for a large number of configurations.

Leaving the initial phase of the mode (0,4) to $\phi_{0,4} = 270°$, which is the most favorable configuration so far, the initial amplitude of the forced modes (0,4) and (0,6) is changed to minimize the pressure peak value of the "target" mode (0,2) in the near-field. Three cases are represented in Fig. 7 for $\varepsilon_{0,4} \times \varepsilon_{0,6} = 5 \times 10^{-10}$, 7×10^{-10}, and 9×10^{-10}. An optimum is reached with $\varepsilon_{0,4} \times \varepsilon_{0,6} = 7 \times 10^{-10}$ where the peak undergoes a decrease of more than 65%.

After paying attention to the initial amplitudes, the same study is conducted on the initial phases of the "killer" modes. As previously the independent initial phase of each mode is not

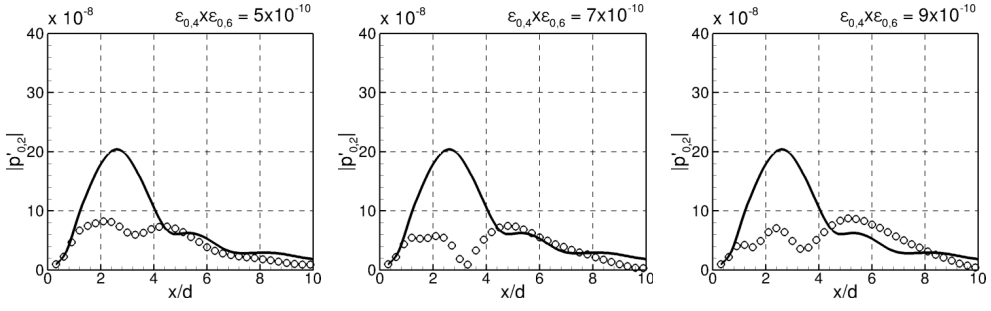

FIG. 7. Pressure amplitude of the "target" mode (0,2) along the line $r/d = 0.5$ when forcing the modes (0,4) and (0,6) with $\phi_{0,4} = 270°$ for various initial amplitude products of the modes (0,4) and (0,6); (∘) nonlinear PSE; (–) linear PSE.

TABLE V. Various initial phases of modes leading to the same results in the near-field. Boldface values refer to the forced modes initial conditions.

Case	$\phi_{0,1}$ ($St = 0.2$)	$\phi_{0,2}$ ($St = 0.4$)	$\phi_{0,3}$ ($St = 0.6$)	$\phi_{0,4}$ ($St = 0.8$)	$\phi_{0,5}$ ($St = 1.0$)	$\phi_{0,6}$ ($St = 1.2$)
E4	0°	0°	0°	**270°**	0°	**0°**
E5	0°	0°	0°	**0°**	0°	**90°**
E6	0°	0°	0°	**225°**	0°	**315°**

essential, it is here the difference of the latter, modulo 2π, which is primordial. Various cases are presented in Table V where the results were equal.

Taking as a starting point, the previous case with $\varepsilon_{0,4} \times \varepsilon_{0,6} = 7 \times 10^{-10}$ where the impact of the nonlinear interactions was the most favorable value, three different phases configurations are reported in Fig. 8 with $\phi_{0,6} - \phi_{0,4} = 85°$, 100°, and 115°. If the discrepancies between the cases are not as large as before, $\phi_{0,6} - \phi_{0,4} = 100°$ leads to a further decrease of the pressure peak value.

F. Effect of the series truncation

As mentioned by Rodriguez *et al.*,[33] nonlinearity couples the evolution of all the frequency and azimuthal wavenumbers. Thus, the arbitrary choice of the highest frequency mode, n_{max}, alters the evolution of any individual mode. For the unforced turbulent jet, these authors conclude that the evolution of higher frequencies is nearly linear. In the present case, where high initial amplitudes are applied to high frequencies, the effect of increasing the truncation frequency has to be investigated and evaluated.

Two cases are considered with different series truncation frequencies, $St = 1.20$ ($n_{max} = 6$) and $St = 2.40$ ($n_{max} = 12$), respectively. In both cases, the previous initial conditions are imposed, that is, to say $\varepsilon_{0,4} \times \varepsilon_{0,6} = 7 \times 10^{-10}$ and $\phi_{0,6} - \phi_{0,4} = 100°$ while all the remaining modes are kept at $\varepsilon_{m,n} = 1 \times 10^{-7}$ and $\phi_{m,n} = 0°$.

The pressure amplitude along the line $r/d = 0.5$ for the first six modes of the computations is reported in Fig. 9. Similarly to the above mentioned unforced turbulent jet, the impact of the truncation frequency on the evolution of lower frequency modes is negligible for the present forced case. In addition, when comparing the nonlinear results with the linear ones, the evolution of higher frequencies is also nearly linear and even for the forced modes. Therefore, the limitation to a finite number of modes will be assumed to have minor impact on the evolution of the modes, even if high initial amplitude is applied on the truncation frequency.

G. Radiated noise

Since the radial extent of the linear-hydrodynamic region varies from one mode to another, a cylindrical Kirchhoff surface has to be determined for each of the modes to propagate the previous results to the far-field.

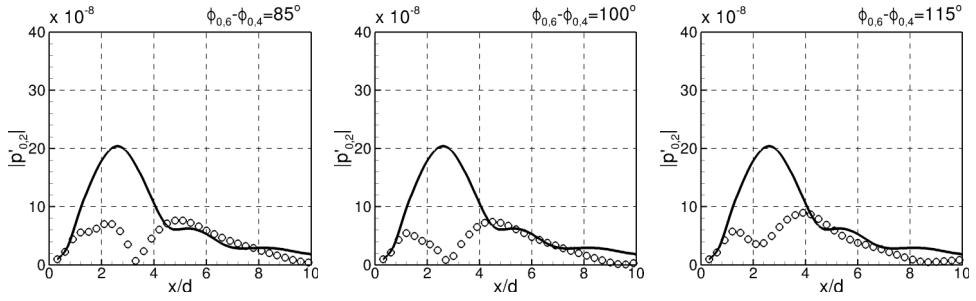

FIG. 8. Pressure amplitude of the "target" mode (0,2) along the line $r/d = 0.5$ when exciting the modes (0,4) and (0,6) at the initial amplitude product $\varepsilon_{0,4} \times \varepsilon_{0,6} = 7 \times 10^{-10}$ for various initial phase differences; (○) nonlinear PSE; (–) linear PSE.

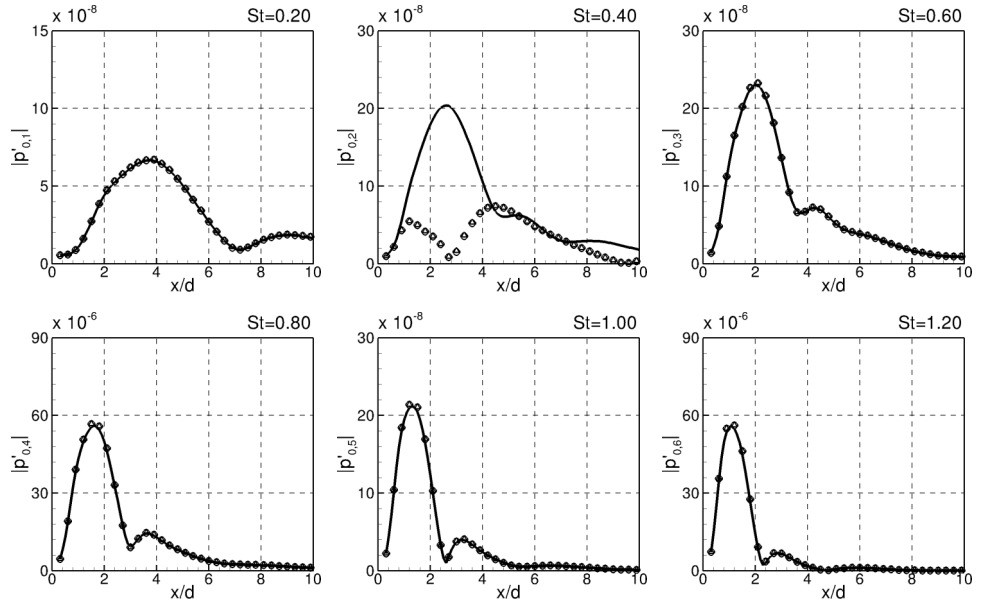

FIG. 9. Series truncation effect (n_{max}) on modes pressure amplitude along the line $r/d = 0.5$ when exciting the modes (0,4) and (0,6) at $\varepsilon_{0,4} \times \varepsilon_{0,6} = 7 \times 10^{-10}$ and $\phi_{0,6} - \phi_{0,4} = 100°$; (○) $n_{max} = 6$; (△) $n_{max} = 12$; (–) linear PSE.

A surface aligned with the x-axis may lead to discrepancies at certain axial locations due to the slow divergence of the jet. Thus, various radial locations of the Kirchhoff surface have been tried out, for each of the modes, on both the unforced and forced jet. Only the acoustic propagation solutions that best match the PSE results along the greater distance in the x-direction have been retained. As an example, both the PSE results (—) and the selected acoustic propagation solution of each mode (- -) at $x/d = 3.0$ are depicted in Figs. 10 and 11 for the unforced and excited jet, respectively.

With the frequency increase, perturbations are damped faster outside of the jet and the location of the Kirchhoff surface has to get closer to the jet. Nevertheless, a limitation to $r_K/d \geq 1.1$ is

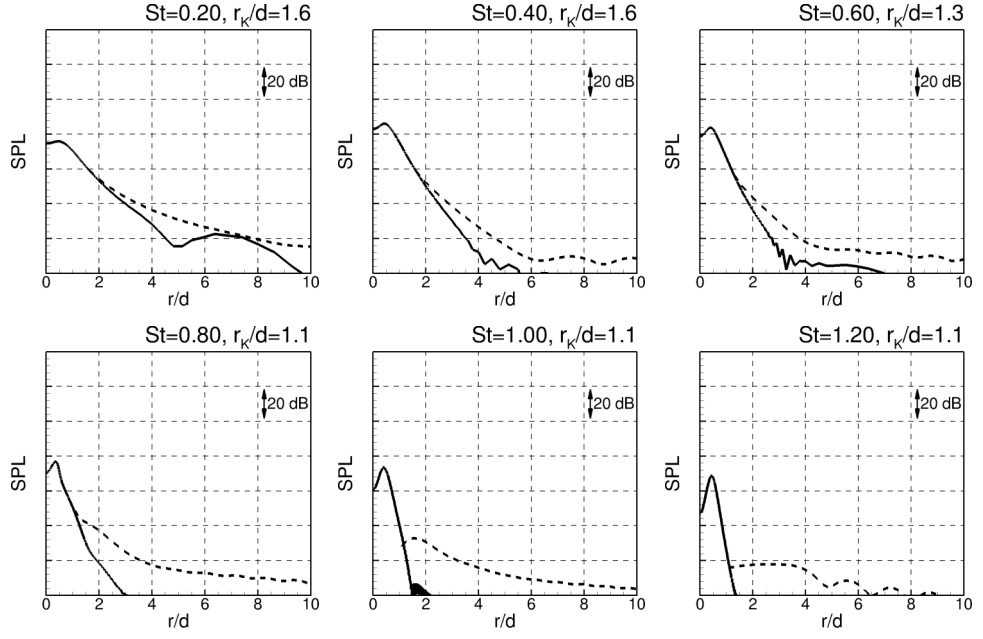

FIG. 10. Near-field radial pressure profile at $x/d = 3.0$ for the unforced jet; PSE (—); acoustic propagation (- -).

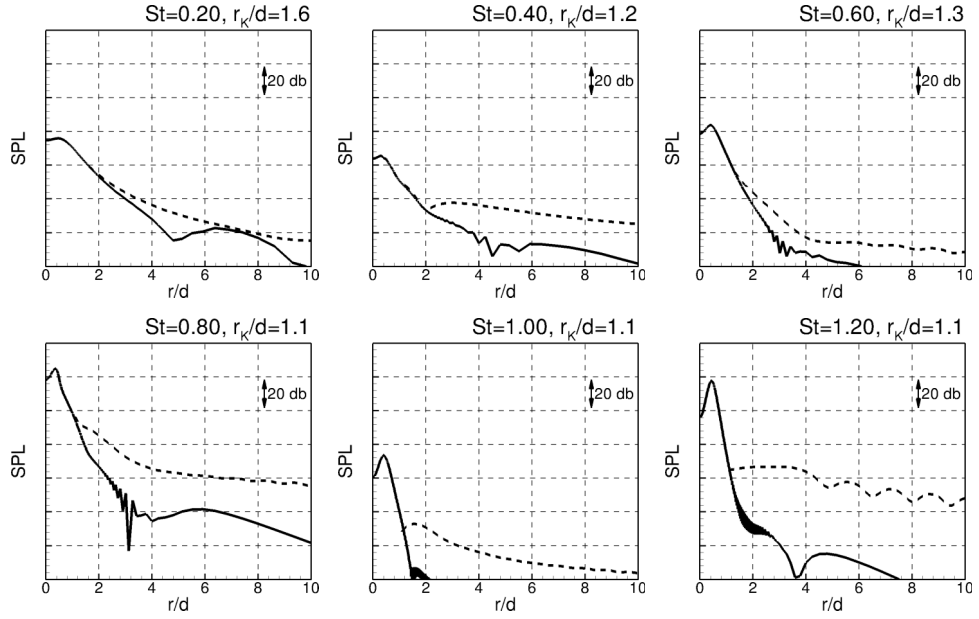

FIG. 11. Near-field radial pressure profiles at $x/d = 3.0$ for the excited jet; PSE (—); acoustic propagation (- -).

imposed on $St \geq 1.00$ to stay outside of the mixing layer and ensure the validity of the Kirchhoff formulation. One can then notice that the propagation of higher frequencies may not be as accurate as expected and thus only an estimate of the acoustic field will be discussed.

Now that the radial location of the Kirchhoff surfaces is determined for each of the modes, the previous results are propagated to the far-field. The pressure field of the "target" mode $St = 0.4$ is depicted in Fig. 12 where two cases are presented, the unforced configuration and the favorable excited conditions mentioned above.

In both cases, the radiating lobe resulting from the hydrodynamic instability is clearly visible with a pronounced directivity in the aft region of the jet. The forcing seems to increase the "target" mode angle of directivity, which moves from 30° to 60°. On the other hand, the pressure levels $|p'_{0,2}|$ are much lower when forcing the difference-frequency mode.

To improve the data analysis, the far-field directivity patterns of the "target" mode are extracted on a circle at $r/d = 25$ from 0° to 90° and are reported in Fig. 13. The three previous combinations of initial phases of the "killer" modes are depicted to quantify the sensitivity to initial conditions,

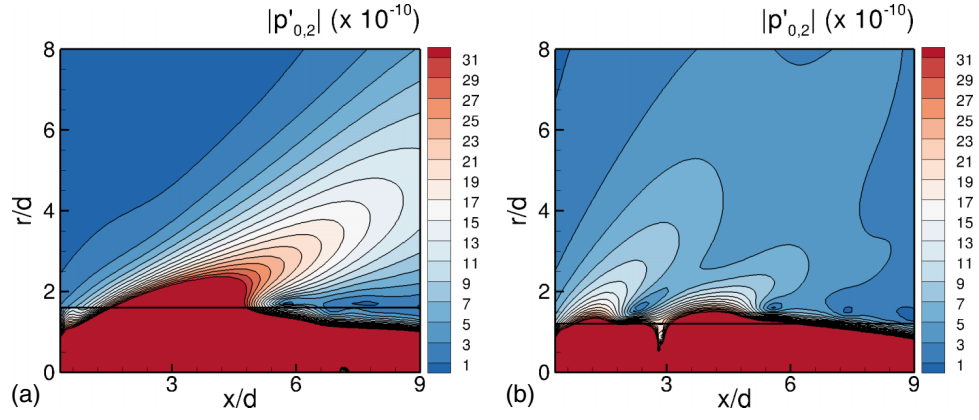

FIG. 12. Pressure field of the "target" mode (0,2) for the unforced jet (a) and for excited jet with the "killer" frequencies $St = 0.80$ and $St = 1.20$ (b); (–) Kirchhoff surface location. (a) Unforced jet. (b) Excited jet.

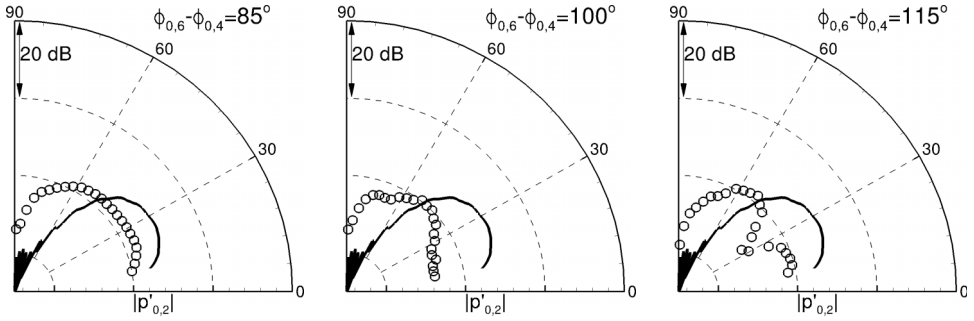

FIG. 13. Pressure level of the mode (0,2) obtained at $r/d = 25$ for various initial phase differences of the modes (0,4) and (0,6) with the initial amplitude product $\varepsilon_{0,4} \times \varepsilon_{0,6} = 7 \times 10^{-10}$; (∘) nonlinear PSE; (–) linear PSE.

so $\phi_{0,6} - \phi_{0,4} = 85°$, 100°, and 115°. A noteworthy change is observed in the angle of directivity and the pressure amplitude of the "target" mode with the initial phase of the "killer" modes. The optimum is found for $\phi_{0,6} - \phi_{0,4} = 100°$ with a significant 9 dB loss of the noise generated by the "target" mode at the frequency $St = 0.40$. It is important to note that the same optimum is found in both the near and far-fields.

However, to decrease the efficiency of the "target" mode, two high frequencies have been amplified and thus may radiate more noise. The overall sound pressure level, which includes all the selected frequencies, is presented in Fig. 14. A noise increase of 33 dB is then highlighted for the forced jet compared to the unexcited jet.

The present results essentially confirm the earlier findings by Suponitsky *et al.*[31] on the idea that nonlinear interaction between two primary instability waves results mainly in a difference frequency mode, but further insight is now provided on the crucial importance of the initial phase of the modes. In fact, when two modes are amplified, low-frequency waves resulting from interactions between primary highly amplified instability waves can be efficient sound radiators in subsonic jets. Nonetheless, and not mentioned in previous work, by carefully setting up amplitudes and phases of two higher frequency modes, the mitigation of the "target" mode noise is possible. On the flip side, the noise induced by the "killer" modes is increased drastically.

H. Shifting to higher frequency "killer" modes

Because outside of the jet high frequencies are damped faster than low frequencies, shifting the "killer" modes to higher frequency is investigated with the aim to reduce the previous increase in the overall sound pressure level.

The exact same process as before is applied, now forcing $St = 1.2$ and $St = 1.6$, instead of $St = 0.8$ and $St = 1.2$. Once more, only the difference-frequency mode, corresponding to $St = 0.4$, is altered while all the other modes are unchanged. An optimum of initial amplitude product is found to be $\varepsilon_{0,6} \times \varepsilon_{0,8} = 7 \times 10^{-10}$. The optimum for the initial phase difference is $\phi_{0,8} - \phi_{0,6} = 115°$.

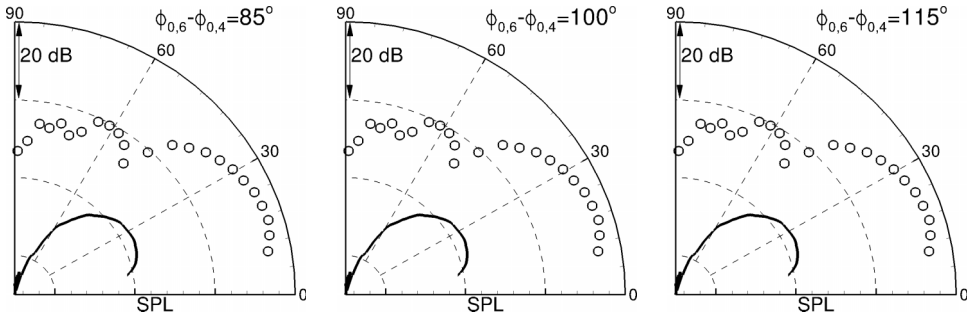

FIG. 14. Overall sound pressure level obtained at $r/d = 25$ for various initial phase sums; (∘) nonlinear PSE; (–) linear PSE.

TABLE VI. Initial amplitudes and phases of modes referring to Fig. 15. Boldface values refer to the forced modes initial conditions.

Case	$\varepsilon_{0,2}$ ($\phi_{0,2}$)	$\varepsilon_{0,6}$ ($\phi_{0,6}$)	$\varepsilon_{0,8}$ ($\phi_{0,8}$)
G1	$1 \times 10^{-7}(0°)$	$\mathbf{2.5 \times 10^{-5}(0°)}$	$\mathbf{2.8 \times 10^{-5}(100°)}$
G2	$1 \times 10^{-7}(0°)$	$\mathbf{2.5 \times 10^{-5}(0°)}$	$\mathbf{2.8 \times 10^{-5}(115°)}$
G3	$1 \times 10^{-7}(0°)$	$\mathbf{2.5 \times 10^{-5}(0°)}$	$\mathbf{2.8 \times 10^{-5}(135°)}$

All the remaining modes, including the "target" mode, are set to initial amplitudes and phases of $\varepsilon_{m,n} = 1 \times 10^{-7}$ and $\phi_{m,n} = 0°$. Once more, as summarized in Table VI, three configurations of initial phase are presented below to quantify sensitivity to initial conditions.

The pressure amplitude of the "target" frequency $St = 0.40$ along the line $r/d = 0.5$ is reported in Figure 15. The efficiency of the process in the near pressure field is obvious in all the three cases with a meaningful lessening of the pressure peak value.

Fig. 16 represents the far-field directivity patterns of the "target" mode at $r/d = 25$. In this case, the forcing seems much more significant in term of noise reduction with a 15 dB loss, instead of 9 dB previously. The results are still sensitive to initial conditions with a loss of 6 dB for other initial phases.

The overall sound pressure level, including the excited frequencies, is presented in Fig. 17. The noise is still increased but by 19 dB, instead of 33 dB previously. Shifting to even higher frequencies may lead to a further decrease, even to a jet noise mitigation. The idea to excite two higher-frequency "killer" modes seems promising by making use of the difference-frequency mode phenomenon. However, a real optimization process must be performed on real initial jet conditions to ensure the feasibility of the process.

I. Nonlinear azimuthal interactions

Instead of pursuing our efforts on axisymmetric modes at even higher frequencies, advantage will be taken of the fact that not only high frequencies but also high azimuthal wavenumbers radiate sound less efficiently, as mentioned by Fuchs and Michel.[49]

A similar investigation is then run on azimuthal interactions. Thirty modes are considered with azimuthal wavenumbers going from −2 to 2 ($m_{max} = 2$) and frequencies ranging from $St = 0.20$ to 1.20 by step of 0.20 ($n_{max} = 6$). The complete routine to minimize the near pressure field is the same as before and will not be detailed. Thereafter, only the main results are presented.

Once more, if single excitation is not relevant with the current purpose, controlling the evolution of a selected "target" mode is made possible through forcing only two "killer" modes (m_1, n_1), (m_2, n_2). In a similar manner than in frequency interactions where the difference-frequency $n_1 - n_2$ was found to predominate, the combination $(m_1 - m_2, n_1 - n_2)$ now prevails over other possible combinations. This is entirely consistent with the analytical model developed by Mankbadi[30] to

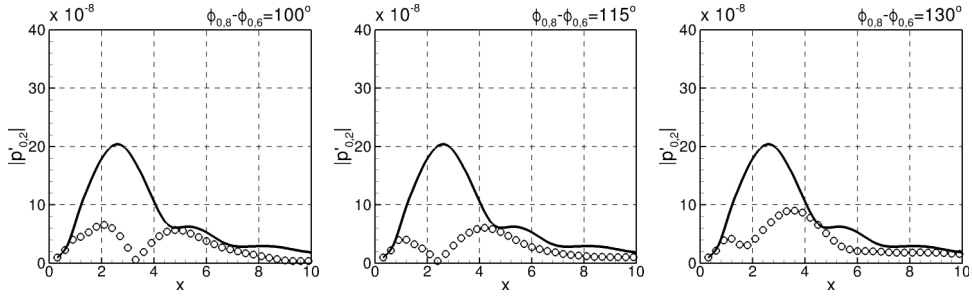

FIG. 15. Pressure amplitude of the "target" mode (0,2) along the line $r/d = 0.5$ when forcing the modes (0,6) and (0,8) at the initial amplitude product $\varepsilon_{0,6} \times \varepsilon_{0,8} = 7 \times 10^{-10}$ for various initial phase differences; (∘) nonlinear PSE; (–) linear PSE.

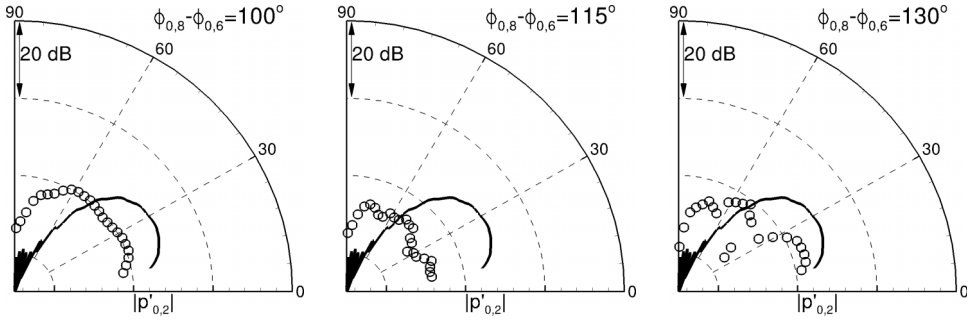

FIG. 16. Pressure level of the mode (0,2) obtained at $r/d = 25$ for various initial phase sums of the modes (0,6) and (0,8) with the initial amplitude product $\varepsilon_{0,6} \times \varepsilon_{0,8} = 7 \times 10^{-10}$; (∘) nonlinear PSE; (–) linear PSE.

study nonlinear wave-wave interactions in turbulent jets. Based on the integrated energy of each scale of motion in a cross section of the jet, he found that two frequency components in the axisymmetric mode can interact with other background frequencies in the axisymmetric mode while two frequency components in a single helical mode cannot, by themselves, amplify other frequency components in the same helical mode. However, combinations of frequency components of helical and axisymmetric modes can amplify other frequencies in other helical modes, which is in agreement with the azimuth and frequency difference phenomena presented here.

The initial amplitude of $\varepsilon_{m,n} = 1 \times 10^{-7}$ remains assigned to all modes while the "killer" modes $(2,4)$ and $(2,6)$ are forced at higher initial amplitudes, thus altering the "target" mode $(0,2)$ corresponding to the axisymmetric mode at the frequency $St = 0.40$.

An optimum in terms of initial amplitudes and phases of the forced modes is sought with the aim of reducing the pressure peak value of the "target" mode. Again, product of initial amplitudes and difference of initial phases are found relevant. The most favorable configuration is got with $\varepsilon_{2,4} \times \varepsilon_{2,6} = 8 \times 10^{-10}$ and $\phi_{2,6} - \phi_{2,4} = 90°$. Pressure amplitude of the "target" mode along the line $r/d = 0.5$ is presented in Fig. 18(a). Again, the pressure peak value of the "target" mode is reduced, supporting the effectiveness of the "target" instability control by "killer" modes.

Far-field directivity pattern of the "target" mode and overall sound pressure obtained at $r/d = 25$ are reported in Figs. 18(b) and 18(c), respectively. As expected by the pressure field, the pressure level of the "target" mode is decreased with a 8 dB loss. Although more favorable than the case presented in Sec. IV G, the overall sound pressure is still increased by 18 dB.

Because the aim of the present paper was to investigate the possibility to control a specific "target" mode, the cost function to minimize was the pressure distribution of the initially dominant instability in the near-field. However, now, the interest must go a step further with a focus on jet noise reduction. Nonetheless, in the range of frequencies and azimuthal wavenumbers selected in the present paper, the initial amplitudes of the "killer" modes needed to influence the initially dominant instability were too high and thus dominate the far-field with always an increase in the overall sound pressure.

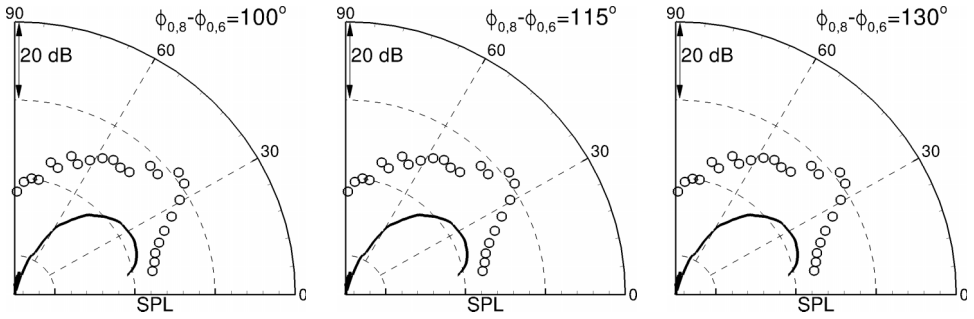

FIG. 17. Overall sound pressure level obtained at $r/d = 25$ for various initial phase sums; (∘) nonlinear PSE; (–) linear PSE.

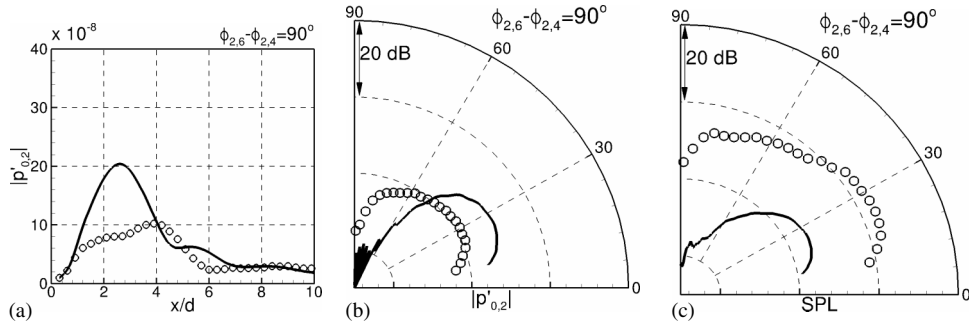

FIG. 18. Pressure amplitude (a) and pressure level (b) of the initially dominant mode (0,2) and overall sound pressure level (c) when forcing the modes (2,4) and (2,6) such that $\varepsilon_{2,4}\times\varepsilon_{2,6}=8\times10^{-10}$ and $\phi_{2,6}-\phi_{2,4}=90°$; (○) nonlinear PSE; linear PSE (–).

But we must still underline that exciting azimuthal modes to impact a given "target" mode development has succeeded. It seems as efficient as amplifying axisymmetric modes of higher frequencies with similar results in terms of pressure distribution and pressure level and thus may be promising even if global jet noise mitigation has not been reached yet.

V. CONCLUSION

PSE approach was used to study nonlinear interactions with forced eigenmodes to control subsonic jet instabilities. Mainly, the objective of the present work was to quantify how modes interact with one another to define proper initial conditions for the recent active control techniques for flow control and noise reduction.

First, the study was restricted to harmonic frequency interactions to clarify the nonlinear underlying mechanism which drives the instabilities evolution. On the one hand, single frequency forcing revealed harmonics growth and thus a broadband jet noise increase. On the other hand, the difference-frequency $n_1 - n_2$ was found to predominate in the near-field when exciting a jet at two frequencies n_1, n_2. This phenomenon was investigated to control the evolution of the initially dominant instability, defined as the "target" mode. The two high frequency forced modes, where energy is injected in order to alter the difference-frequency mode behavior, were qualified as "killer" modes. Of particular interest were the initial conditions of the "killer" modes. Not only their initial amplitudes were found critical for the "target" mode development but also their initial phases. Specifically, the product of the "killer" mode initial amplitudes and the difference of their initial phases were key parameters. An optimum was found with the objective of minimizing the near-field pressure peak value of the "target" frequency. The propagation of that PSE solution to the far-field revealed a significant decrease of the initially dominant instability noise with a 15 dB loss. However, the "killer" modes dominate in the far-field due to their needed high initial amplitudes. As a result, the estimated overall sound pressure level was increased by 19 dB. A solution proposed to reduce that drastic increase of the overall sound pressure level is to shift the "killer" modes to even higher frequencies, which are damped faster outside of the jet.

Then, because high azimuthal wavenumbers also radiate sound less efficiently, the same overall process was realized on azimuthal modes. As an extension of the difference-frequency, it was found that amplifying two "killer" modes (m_1,n_1), (m_2,n_2) influences the combination $(m_1 - m_2, n_1 - n_2)$. This result was found to be fully in line with the analytical model developed by Mankbadi.[30] Once more, the behavior of the initially dominant instability was investigated as a function of the initial conditions of the two "killer" modes. Once again, although the needed initial amplitudes of the "killer" modes were too high and thus led to an increase in the overall sound pressure, the near pressure field as well as the radiated noise of the naturally dominant instability were remarkably reduced. It should be noted that in all three cases mentioned previously, the optimal phase difference is found to be around 100°. To the best of our knowledge, the underlying mathematics or physics, which might explains why that is, remains an open question.

In return for a frequency-shift in noise, the present paper supports the approach that the noise mitigation of the initially dominant instability is feasible by means of nonlinear frequency interactions. In addition, sometimes a specific frequency related to jet instabilities may dominate the entire spectrum, which can be harmful or dangerous for the aircraft structure. To prevent such issues, this process might be an appropriate solution.

[1] M. Lighthill, "On sound generated aerodynamically. I. General theory," Proc. R. Soc. London, Ser. A **211**, 564–587 (1952).
[2] R. Franklin and J. Foxwell, "Correlation in the random pressure field close to a jet," Technical Report No. 3161, Aeronautical Research Council, 1958.
[3] P. Bradshaw, D. Ferriss, and R. Johnson, "Turbulence in the noise producing region of a circular jet," J. Fluid Mech. **19**, 591–624 (1964).
[4] E. Mollo-Christensen, M. Kolpin, and J. Martuccelli, "Experiments on jet flows and jet noise far-field spectra and directivity patterns," J. Fluid Mech. **18**, 285–301 (1964).
[5] S. Crow and F. Champagne, "Orderly structure in jet turbulence," J. Fluid Mech. **48**, 547–591 (1971).
[6] D. Crighton and P. Huerre, "Shear-layer pressure fluctuations and superdirective acoustic sources," J. Fluid Mech. **220**, 355–368 (1990).
[7] A. Cavalieri, P. Jordan, A. Agarwal, and Y. Gervais, "Jittering wave-packet models for subsonic jet noise," J. Sound Vib. **330**, 4474–4492 (2011).
[8] A. Cavalieri and A. Agarwal, "Coherence decay and its impact on sound radiation by wavepackets," J. Fluid Mech. **748**, 399–415 (2014).
[9] C. Tam, "Jet noise: Since 1952," Theor. Comput. Fluid Dyn. **10**, 393–405 (1998).
[10] T. Colonius and S. Lele, "Computational aeroacoustics: Progress on nonlinear problems of sound generation," Prog. Aeronaut. Sci. **40**, 345–416 (2004).
[11] P. Jordan and Y. Gervais, "Subsonic jet aeroacoustics: Associating experiment, modelling and simulation," Exp. Fluids **44**, 1–21 (2008).
[12] T. Suzuki and T. Colonius, "Instability waves in a subsonic round jet detected using a near-field phased microphone array," J. Fluid Mech. **565**, 197–226 (2006).
[13] A. Cavalieri, G. Daviller, P. Comte, P. Jordan, G. Tadmor, and Y. Gervais, "Using large eddy simulation to explore sound-source mechanisms in jets," J. Sound Vib. **330**, 4098–4113 (2011).
[14] J. Nichols and S. Lele, "Global modes and transient response of a cold supersonic jet," J. Fluid Mech. **669**, 225–241 (2011).
[15] F. Bertolotti and T. Herbert, "Analysis of the linear stability of compressible boundary layers using the PSE," Theor. Comput. Fluid Dyn. **3**, 117–124 (1991).
[16] P. Balakumar, "Prediction of supersonic jet noise," AIAA Paper No. 98-1057, 1998.
[17] C. Yen and N. Messersmith, "Application of parabolized stability equations to the prediction of jet instabilities," AIAA J. **36**, 1541–1544 (1998).
[18] F. Bertolotti and T. Colonius, "On the noise generated by convected structures in a Mach 0.9, hot, turbulent jet," AIAA Paper 2003-1062, 2003.
[19] E. Piot, G. Casalis, F. Muller, and C. Bailly, "Investigation of the PSE approach for subsonic and supersonic hot jets. Detailed comparisons with LES and linearized Euler equations results," Int. J. Aeroacoust. **5**, 361–393 (2006).
[20] K. Gudmundsson, "Instability wave models of turbulent jets from round and serrated nozzles," Ph.D. thesis, California Institute of Technology, 2010.
[21] K. Gudmundsson and T. Colonius, "Instability wave models for the near-field fluctuations of turbulent jets," J. Fluid Mech. **689**, 97–128 (2011).
[22] O. Léon, "Étude du rayonnement acoustique des instabilités hydrodynamiques de jets double-flux avec les équations de stabilité parabolisées (PSE)," Ph.D. thesis, Université de Toulouse, 2012.
[23] O. Léon and J.-P. Brazier, "Investigation of the near and far pressure fields of dual-stream jets using an Euler-based PSE model," AIAA Paper 2013-2280, 2013.
[24] M. Samimy, J. Kim, J. Kastner, I. Adamovich, and Y. Utkin, "Active control of high-speed and high-Reynolds-number jets using plasma actuators," J. Fluid Mech. **578**, 305–330 (2007).
[25] M. Kearney-Fischer, J.-H. Kim, and M. Samimy, "A study of Mach wave radiation using active control," J. Fluid Mech. **681**, 261–292 (2011).
[26] G. Raman, E. Rice, and R. Mankbadi, "Saturation and the limit of jet mixing enhancement by single frequency plane wave excitation: Experiment and theory," AIAA Paper No. 88-3613, 1988.
[27] D. Ronneberger and U. Ackermann, "Experiments on sound radiation due to non-linear interaction of instability waves in a turbulent jet," J. Sound Vib. **62**, 121–129 (1979).
[28] H. Arbey and J. Ffowcs Williams, "Active cancellation of pure tones in an excited jet," J. Fluid Mech. **149**, 445–454 (1984).
[29] G. Raman and E. Rice, "Axisymmetric jet forced by fundamental and subharmonic tones," AIAA J. **29**, 1114–1122 (1991).
[30] R. Mankbadi, "Multifrequency excited jets," Phys. Fluids A **3**, 595–605 (1991).
[31] V. Suponitsky, N. Sandham, and C. Morfey, "Linear and nonlinear mechanisms of sound radiation by instability waves in subsonic jets," J. Fluid Mech. **658**, 509–538 (2010).
[32] V. Kopiev, I. Belyaev, M. Zaytsev, V. Kopiev, and G. Faranosov, "Acoustic control of instability waves in a turbulent jet," Acoust. Phys. **59**, 16–26 (2013).
[33] D. Rodriguez, A. Samanta, A. Cavalieri, T. Colonius, and P. Jordan, "Parabolized stability equation models for predicting large-scale mixing noise of turbulent round jets," AIAA Paper 2011-2838, 2011.
[34] M. Malik and C. Chang, "Nonparallel and nonlinear stability of supersonic jet flow," Comput. Fluids **29**, 327–365 (2000).
[35] L. Cheung, D. Bodony, and S. Lele, "Noise radiation predictions from jet instability waves using a hybrid nonlinear PSE-acoustic analogy approach," AIAA Paper 2007-3638, 2007.

[36] M. Huet, "Influence of boundary layers resolution on heated, subsonic, high Reynolds number jet flow and noise," AIAA Paper 2013-2141, 2013.
[37] P. Monkewitz and K. Sohn, "Absolute instability in hot jets," AIAA J. **26**, 911–916 (1988).
[38] H. Haj-Hariri, "Characteristics analysis of the parabolized stability equations," Stud. Appl. Math. **92**, 41–53 (1994). For more information, go to http://cat.inist.fr/?aModele=afficheN&cpsidt=3348892.
[39] Y. Vigneron, J. Rakich, and J. Tannehill, "Calculation of supersonic viscous flow over delta wings with sharp subsonic leading edges," AIAA Paper No. 78-1137, 1978.
[40] L. Gamet, F. Ducros, F. Nicoud, and T. Poinsot, "Compact finite difference schemes on non-uniform meshes. Application to direct numerical simulations of compressible flows," Int. J. Numer. Methods Fluids **29**, 159–191 (1999).
[41] O. Léon and J.-P. Brazier, "Application of the linear parabolized stability equations to a subsonic coaxial jet," AIAA Paper 2011-2839, 2011.
[42] K. Gudmundsson and T. Colonius, "Parabolized stability equation models for turbulent jets and their radiated sound," AIAA Paper 2009-3380, 2009.
[43] J. Brazier, M. Huet, O. Léon, and M. Itasse, "Modal analysis of near-field pressure fluctuation for a cold subsonic jet," in 50th AAAF International Conference: Applied Aerodynamics, 2015.
[44] T. Troutt and D. McLaughlin, "Experiments on the flow and acoustic properties of a moderate-Reynolds-number supersonic jet," J. Fluid Mech. **116**, 123–156 (1982).
[45] F. Muller, F. Vuillot, G. Rahier, G. Casalis, and E. Piot, "Experimental and numerical investigation of the near field pressure of a high subsonic hot jet," AIAA Paper 2006-2535, 2006.
[46] S. Bagheri, P. Schlatter, P. Schmid, and D. Henningson, "Global stability of a jet in crossflow," J. Fluid Mech. **624**, 33–44 (2009).
[47] A. Salgado, A. Agarwal, V. Suponitsky, and N. Sandham, "A non-linear PSE-based model for jet noise," AIAA Paper 2010-3969, 2010.
[48] D. Bechert and E. Pfizenmaier, "On the amplification of broad band jet noise by a pure tone excitation," J. Sound Vib. **43**, 581–587 (1975).
[49] H. Fuchs and U. Michel, "Experimental evidence of turbulence source coherence affecting jet noise," AIAA J. **16**, 871–872 (1978).